THE JOURNAL OF PHYSICAL CHEMISTRY Letters

Letter

pubs.acs.org/JPCL

# Reproducible Deep-UV SERRS on Aluminum Nanovoids

Daniel O. Sigle,[†] Elaine Perkins,[‡] Jeremy J. Baumberg,*[,†] and Sumeet Mahajan*[,†,#]

[†]Cavendish Laboratory, University of Cambridge, Cambridge CB3 0HE, United Kingdom

[‡]Dstl Porton Down, Salisbury SP4 0JQ, United Kingdom

Supporting Information

**ABSTRACT:** Surface-enhanced Raman scattering (SERS) with deep-UV excitation is of particular interest because a large variety of biomolecules such as amino acids exhibit electronic transitions in the UV spectral range and resonant excitation dramatically increases the cross section of the associated vibrational modes. Despite its potential, UV-SERS is still little-explored. We present a novel straightforward scalable route to fabricate aluminum nanovoids for reproducible SERS in the deep-UV without the need of expensive lithographic techniques. We adopt a modified template stripping method utilizing a soluble template and self-assembled polymer spheres to create nanopatterned aluminum films. We observe high surface enhancement of approximately 6 orders of magnitude, with excitation in the deep-UV (244 nm) on structures optimized for this wavelength. This work thus enables sensitive detection of organics and biomolecules, normally nonresonant at visible wavelengths, with deep-UV surface-enhanced resonant Raman scattering on reproducible and scalable substrates.

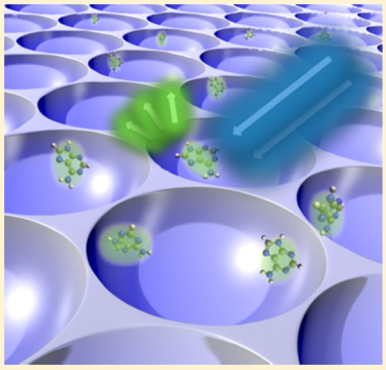

**SECTION:** Plasmonics, Optical Materials, and Hard Matter

Since the discovery of surface-enhanced Raman scattering in the 1970s,[1−3] this technique has been improved in many ways and is now a powerful method to determine the composition of a large variety of substances. To date, the most commonly used excitation wavelengths are in the visible and near-infrared (NIR) spectral ranges. On the other hand, excitation in the deep-UV (<300 nm) allows combination of surface enhancement with resonant enhancement of a large number of molecules through surface-enhanced resonant Raman scattering (SERRS).[4] This opens up numerous exciting possibilities such as the study of photoinduced reactions and detection of biomolecules such as DNA and proteins in their native state at low concentrations, highly sought after for biochemical characterization. Excitation in the deep-UV also increases the spatial resolution while the fluorescent background is simultaneously reduced as most molecules do not fluoresce in the deep-UV.[5]

SERS detection requires the use of metallic nanostructures such as nanoparticles[6] or nanostructured surfaces to excite a surface plasmon resonance. Both of these have been utilized extensively, but for portable and high-throughput detection strategies, the latter have proved highly suitable. For widespread use of SERS detection techniques, a key requirement is the reproducibility of the spectra, which critically depends on the fabrication tolerances of the nanostructured surface.[7] Although there has been considerable research on SERS substrates, only a few of them actually demonstrate reproducible spectra.[8−10] Despite the potential of SERS in the deep-UV, no such substrate is commercially available for this wavelength regime.

Here, we present a novel route to fabricate aluminum nanovoid surfaces for SERS in the deep-UV in a straightforward and inexpensive way. In contrast to gold and silver, aluminum has weak optical absorption down to wavelengths of 200 nm and is capable of supporting surface plasmons in the UV.[11−15] Nanovoids have proven to be an attractive substrate due to their highly reproducible geometry as well as their high electromagnetic enhancement with robust fabrication tolerance and have been fabricated by electrodepositing metals such as gold, silver, or palladium around a template layer of polymer nanospheres.[16−19] However, electrodeposition of aluminum is particularly complicated and only possible from ionic liquids.[20] Our alternative route utilizes self-assembled colloidal sphere templates, combined with the ease of physical vapor deposition and template stripping. Avoiding electrochemical techniques for the fabrication improves the simplicity and scalability of this route for commercial production. Template stripping of metal films has mostly been demonstrated on substrates such as mica[21] and silicon[22] with noble metals such as gold and silver, which can be released from the template directly, owing to the different crystalline structure of the two phases and weak adhesion. Aluminum, however, forms strong bonds with silicon; therefore, direct template stripping is not possible, and long-chain fluorinated silane spacers or release layers need to be used.[23] We eliminate this additional complexity by using a fully dissolvable template. Furthermore, although deep-UV SERS has been reported on evaporated aluminum films,[24] on aluminum nanoparticle arrays,[25] on bow-tie antennas,[26] and in tip-enhanced Raman scattering (TERS) experiments,[27] none of these structures are measured to give reproducible signals. In

**Received:** March 4, 2013
**Accepted:** April 9, 2013
**Published:** April 9, 2013

   dx.doi.org/10.1021/jz4004813 | J. Phys. Chem. Lett. 2013, 4, 1449−1452

this work, we optimize our aluminum nanovoid structures to give ~$10^6$ surface enhancement and study their plasmonic properties. Thus, our work paves the way for widespread utilization of UV-SERRS substrates for sensitive detection of biomolecules.

PMMA sheets (GoodFellow) were rinsed in ethanol and water. Colloidal polystyrene spheres (Thermo Scientific) were mixed with ethanol to increase the wettability and spread over the PMMA sheet by spin coating, where they form a monolayer via self-assembly. We prepared a range of samples using sphere diameters between 100 and 500 nm. Subsequently, a layer of aluminum (Kurt Lesker, purity 99.99%) was deposited onto the spheres via electron beam evaporation. The aluminum deposition speed is critical. Fast deposition increases the amount of heat transferred to the template spheres and causes partial melting. This leads to corrugations on the void surface. Therefore, we initially used a slow deposition rate of 0.1 Å/s for the first 5 nm, subsequently increased it to 0.5 Å/s for the next 15 nm, and finally set to a value of 1 Å/s until a thickness of 400 nm was reached. A polyimide tape (Onecall) was then secured on top of the aluminum film, and the PMMA and template spheres underneath were dissolved in THF, and the sample was rinsed in water. The void structure is obtained on the bottom side of the evaporated film. The voids are almost perfect hemispherical cavities with short pillars at the interstices of the three touching template beads. The cavity size corresponds directly to the diameter of the polymer nanosphere used for template formation. Figure 1 depicts the fabrication process and the obtained pattern found by scanning electron microscopy (SEM). For SERS measurements, the substrate was fixed on a glass slide.

For Raman and SERS measurements, we used a Renishaw inVia Raman microscope. The UV excitation light had a wavelength of 244 nm and was provided by a frequency-doubled 488 nm argon ion laser. The laser spot size was 5 $\mu$m, and the optical power density on the sample was 1500 W/cm$^2$. The exposure time was 30 s, and 10 acquisitions were performed for each spectrum. We used an objective with 40× magnification (OFR LMU-40x) and a numerical aperture of 0.5. The setup included a 3600 lines/mm grating and provided a spectral resolution of 6 cm$^{-1}$. For NIR SERS, we used a 785 nm diode laser source and a 1200 lines/mm grating.

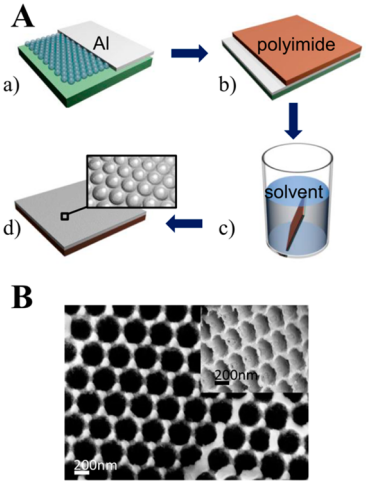


**Figure 1.** (A) Fabrication of the nanovoid films: (a) Deposition of a monolayer of polystyrene template beads on a PMMA substrate via spin coating, followed by slow evaporation of aluminum on the template; (b) A polyimide sheet was placed on top of the aluminum film. (c) The PMMA layer and polystyrene beads were dissolved in THF. (d) The void pattern was obtained on the bottom side of the aluminum film. (B) SEM of the voids: top view and view at 45° (inset).

Aluminum nanovoid substrates were prepared as described above. We used adenine in a 1 mM aqueous solution as our interrogation molecule. A small droplet was placed on the substrate and covered with a quartz coverslip. In order to avoid molecular photodegradation, SERS measurements were performed in wet conditions. This ensures constant coverage of the nanovoid surface as molecules are constantly replenished by diffusive flows. Calibration Klarite substrates for SERS with NIR excitation were obtained from Renishaw Diagnostics.

For simulations, we used Lumerical 7.5, a commercial FDTD Maxwell solver. Due to computational complexity, we only modeled a single void rather than a hexagonal array, which we have previously shown captures the essential plasmonic modes.[15−18]

Aluminum nanovoid substrates on polyimide films were used for UV-SERRS measurements. Figure 2A,a depicts a typical

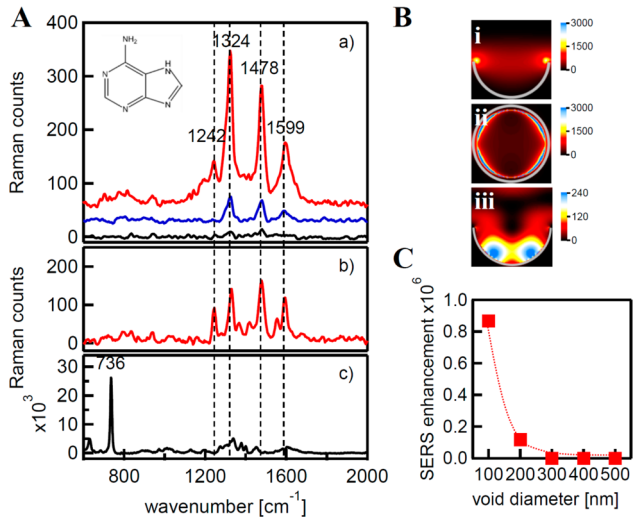


**Figure 2.** (A) (a) UV-SERRS spectrum of a 1 mM adenine solution on a 200 nm void structured aluminum surface (red) compared to the UV-SERRS spectrum on an evaporated aluminum surface (blue) and the resonant Raman spectrum of adenine solution without a plasmonic surface (black). The inset shows the structure formula of adenine. (b) UV resonant Raman spectrum of bulk adenine in powder form. (c) NIR SERS spectrum (excitation 785 nm) of adenine solution on Klarite. (B) Field intensity ($|E|^2$) in the void for a 100 nm cavity: (i) cross section and (ii) the view from the top. The field is concentrated in a small volume near the rim. (iii) Intensity in a 200 nm cavity with an additional mode deeper inside of the void (the volume mode). (C) SERRS enhancement in the enhanced field region on voids for increasing void diameters. The dashed line is a guide for the eye.

UV-SERRS spectrum of adenine obtained on an aluminum nanovoid surface (red spectrum) with a 200 nm cavity diameter. We took many spectra on three different substrates for each void size and found variations of the peak heights of 15% (see Figure S1 in the Supporting Information). We believe that this reproducibility is limited mainly by lattice defects occurring during the self-assembly process. Nevertheless, in the context of various alternative SERS-active geometries, this value signifies good spectral reproducibility. Adenine peaks are also observed but are much weaker on an aluminum film evaporated


dx.doi.org/10.1021/jz4004813 | J. Phys. Chem. Lett. 2013, 4, 1449−1452

on a silicon wafer (blue spectrum) due to its inherent roughness and the resonance enhancement of the molecule. Very small but unclear peaks are observed for the adenine solution without any aluminum surface (black) due to resonance enhancement alone. The resonant Raman spectrum of adenine powder (Figure 2A,b) and the nonresonant SERS of 1 mM adenine solution at 785 nm excitation on Klarite (Figure 2A,c) are shown for comparison. We note that in the nonresonant SERS spectrum with 785 nm excitation (Figure 2A,c), the most prominent peak is at 736 $cm^{-1}$, while in the UV, the bands at around 1300 $cm^{-1}$ are much stronger. These are mostly the in-plane stretching modes of several C−N bonds. While relative changes in intensity of different peaks are usually attributed to orientation changes, the absence of the 736 $cm^{-1}$ mode suggests the role of resonance enhancement to account for the differences between aluminum nanovoid and gold Klarite surfaces. The peaks between 1242 and 1600 $cm^{-1}$ are resonantly enhanced due to the delocalized character of the involved electrons as they are in-plane stretching modes and will be aligned with the electronically excited transition dipole. The peaks at 736 and 630 $cm^{-1}$ are ring breathing and deformation modes,[28] respectively. They will not be affected by excitation of the molecular dipole and therefore do not undergo resonance enhancement. Additionally, charge-transfer mechanisms can contribute to the stronger enhancement of the bands between 1242 and 1600 $cm^{-1}$ under UV excitation.[29]

In order to optimize our substrate for deep-UV excitation, we tested a range of different void diameters between 100 and 500 nm. High SERRS signals were obtained with 100 and 200 nm cavities, while larger voids do not show significant improvement over the rough aluminum surface. We measured an average enhancement factor of 100 for the 200 nm void and 60 on the 100 nm void. In order to understand the geometry of the "hot-spot regions" in these two cases, we simulated a hemispherical aluminum nanovoid using Lumerical. In the case of the 100 nm voids, the field is concentrated in only a small volume in the proximity of the rim region (Figure 2B, i and ii). In the 200 nm cavity, the magnitude of the field in the rim region is much weaker, but an additional mode occurs deeper inside the void (Figure 2B,iii). We denote the two different modes as the rim mode and volume mode, respectively.[30] Due to the stronger localization of the field in the 100 nm void into a small volume, the number of molecules contributing to the SERS signal is much smaller, and the effective enhancement is significantly higher (see also the Supporting Information). Figure 2C depicts the observed surface-enhancement dependence in the enhanced field region on the void diameter, which is almost 6 orders of magnitude on the 100 nm void.

We further observe shifts of the UV-SERRS peaks compared to those of the resonant Raman spectrum of bulk adenine. The most prominent peak is shifted from 1333 $cm^{-1}$ in the bulk Raman spectrum compared to 1324 $cm^{-1}$ in the SERRS spectrum. The peak at 1478 $cm^{-1}$ is not shifted, while the third peak is shifted to higher wavenumbers from 1593 to 1599 $cm^{-1}$. The direction of the shift is governed by the interaction of the respective molecular dipole with the metallic surface. We also note differences in the ratios of the three prominent peaks (1324, 1478, and 1599 $cm^{-1}$) in the respective SERRS spectra (see Figure S1 in the Supporting Information). In particular, the band at 1599 $cm^{-1}$ is more prominent in the case of the 100 nm void. We attribute this to the spatial location of the high field enhancement regions inside this structure.

In the case of the volume mode for the 200 nm cavity, the Raman-enhanced molecules do not have to be as near the surface and hence have reduced interaction with it. In the case of the rim mode for the smaller nanovoids, the field is highest near the surface; therefore, the molecules contributing to the SERRS spectra have substantial interaction with the surface. Hence, the observed differences in SERRS intensity and peak position between the two void sizes stem from the fact that the SERRS in the two cases is reported from different regions of the nanovoid architecture and thus directly relates to the differences in the nature of the supported plasmon modes.

In order to characterize the plasmonic response of the system and further understand the observed enhancements, we modeled the extinction spectrum for varying void diameters. The red dashed line and the blue dashed line in Figure 3

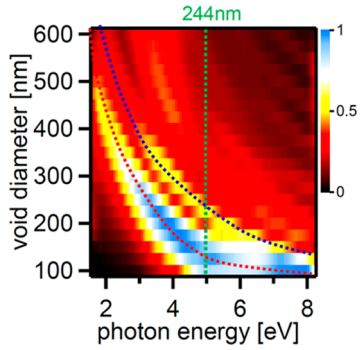


**Figure 3.** Simulated optical extinction of aluminum nanovoids with different diameters at normal incidence in aqueous media. The location of the rim mode and volume mode is indicated by red and blue dashed lines, respectively. The green dashed line indicates the Raman excitation wavelength. The highest plasmonic activity at 244 nm is achieved for a void diameter of 125 nm.

indicate the rim mode and the volume mode, respectively. Excited at 244 nm, the Raman excitation line, the 100 nm void exhibits the highest plasmonic activity indicated by the highest optical absorption in this range. The plasmon mode on the 100 nm void is further red-shifted by ∼0.6 eV due to the natural oxide layer on aluminum (see Figure S2 in the Supporting Information). However, overall, we find that surface oxidation does not dramatically change the SERRS on such aluminum nanovoids. The SERS activity decreases with increasing size of the void, and with larger voids (>400 nm), negligible absorption is seen. This correlates well with the observed SERRS enhancements.

We present a straightforward novel route to fabricate aluminum nanovoids without the need for complex electrochemistry or lithographic methods. Our approach uses a modified template stripping technique with a soluble backing layer to fabricate aluminum nanovoids. The simplicity of the techniques involved makes this approach scalable and suitable for large-scale production. It caters to the current lack of availability of commercial substrates for deep-UV SERS. We studied SERRS on these aluminum nanovoid surfaces and found that with appropriate geometries, high enhancements (∼$10^6$) over and above resonance enhancements are observed. We further electromagnetically simulated our aluminum hemispherical nanovoids in order to understand the observed SERRS spectra and enhancements. Our results show that nanostructured aluminum surfaces are indeed able to support significant plasmonic activity, which leads to high enhance-


dx.doi.org/10.1021/jz4004813 | J. Phys. Chem. Lett. 2013, 4, 1449−1452

ments with deep-UV SERRS. We find that the natural oxide layer only marginally affects the enhancements within this geometry.

## ■ ASSOCIATED CONTENT

### Supporting Information

Comparison of spectra on 100 nm voids and 200 nm voids, calculation of enhancement factors, and simulation of the impact of the oxide layer. This material is available free of charge via the Internet at http://pubs.acs.org.

## ■ AUTHOR INFORMATION


### Corresponding Author

*E-mail: jjb12@cam.ac.uk (J.J.B.); sm735@cam.ac.uk (S.M.).

### Present Address

[#]S.M.: Institute of Life Sciences, University of Southampton, Highfield, Southampton SO17 1BJ, U.K.


### Notes

The authors declare no competing financial interest.

## ■ ACKNOWLEDGMENTS

This work was supported by the Defence Science and Technology Laboratory (DSTL) and EPSRC Grant EP/G060649/1. We thank Renishaw Diagnostics for providing Klarite substrates.

## ■ REFERENCES


(1) Fleischmann, M.; Hendra, P. J.; McQuillan, A. J. Raman Spectra of Pyridine Adsorbed at a Silver Electrode. *Chem. Phys. Lett.* **1974**, *26*, 163−166.

(2) Albrecht, G.; Creighton, A. Anomalously Intense Raman Spectra of Pyridine at a Silver Electrode. *J. Am. Chem. Soc.* **1977**, *99*, 5215−5217.

(3) Jeanmaire, D. L.; Van Duyne, R. P. Surface Raman Spectroelectrochemistry: Part I. Heterocyclic, Aromatic, and Aliphatic Amines Adsorbed on the Anodized Silver Electrode. *J. Electroanal. Chem. Interfacial Electrochem.* **1977**, *84*, 1−20.

(4) Asher, S. A. UV Resonance Raman Spectroscopy for Analytical, Physical, and Biophysical Chemistry. Part 1. *Anal. Chem.* **1993**, *65*, 59A−66A.

(5) Kämmer, E.; Dörfer, T.; Csáki, A.; Schumacher, W.; Da Costa Filho, P. A.; Tarcea, N.; Fritzsche, W.; Rösch, P.; Schmitt, M.; Popp, J. Evaluation of Colloids and Activation Agents for Determination of Melamine Using UV-SERS. *J. Phys. Chem. C* **2012**, *116*, 6083−6091.

(6) Cui, L.; Wang, A.; Wu, D.-Y.; Ren, B.; Tian, Z.-Q. Shaping and Shelling Pt and Pd Nanoparticles for Ultraviolet Laser Excited Surface-Enhanced Raman Scattering. *J. Phys. Chem. C* **2008**, *112*, 17618−17624.

(7) Lin, X.-M.; Cui, Y.; Xu, Y.-H.; Ren, B.; Tian, Z.-Q. Surface-Enhanced Raman Spectroscopy: Substrate-Related Issues. *Anal. Bioanal. Chem.* **2009**, *394*, 1729−45.

(8) Mahajan, S.; Abdelsalam, M.; Suguwara, Y.; Cintra, S.; Russell, A.; Baumberg, J.; Bartlett, P. Tuning Plasmons on Nano-structured Substrates for NIR-SERS. *Phys. Chem. Chem. Phys.* **2007**, *9*, 104−109.

(9) Misra, A. K.; Sharma, S. K.; Kamemoto, L.; Zinin, P. V; Yu, Q.; Hu, N.; Melnick, L. Novel Micro-Cavity Substrates for Improving the Raman Signal from Submicrometer Size Materials. *Appl. Spectrosc.* **2009**, *63*, 373−377.

(10) Mahajan, S.; Baumberg, J. J.; Russell, A. E.; Bartlett, P. N. Reproducible SERRS from Structured Gold Surfaces. *Phys. Chem. Chem. Phys.* **2007**, *9*, 6016−6020.

(11) Ekinci, Y.; Solak, H. H.; David, C. Extraordinary Optical Transmission in the Ultraviolet Region through Aluminum Hole Arrays. *Opt. Lett.* **2007**, *32*, 172−174.

(12) Ekinci, Y.; Solak, H. H.; Loffler, J. F. Plasmon Resonances of Aluminum Nanoparticles and Nanorods. *J. Appl. Phys.* **2008**, *104*, 83106−83107.

(13) Mattiucci, N.; D'Aguanno, G.; Everitt, H. O.; Foreman, J. V; Callahan, J. M.; Buncick, M. C.; Bloemer, M. J. Ultraviolet Surface-Enhanced Raman Scattering at the Plasmonic Band Edge of a Metallic Grating. *Opt. Express* **2012**, *20*, 1868−1877.

(14) Chan, G. H.; Zhao, J.; Schatz, G. C.; Van Duyne, R. P. Localized Surface Plasmon Resonance Spectroscopy of Triangular Aluminum Nanoparticles. *J. Phys. Chem. C* **2008**, *112*, 13958−13963.

(15) Langhammer, C.; Schwind, M.; Kasemo, B.; Zoric, I. Localized Surface Plasmon Resonances in Aluminum Nanodisks. *Nano Lett.* **2008**, *8*, 1461−1471.

(16) Cole, R. M.; Baumberg, J. J.; De Abajo, F. J.; Mahajan, S.; Abdelsalam, M.; Bartlett, P. N. Understanding Plasmons in Nanoscale Voids. *Nano Lett.* **2007**, *7*, 2094−2100.

(17) Coyle, S.; Netti, M. C.; Baumberg, J. J.; Ghanem, M. A.; Birkin, P. R.; Bartlett, P. N.; Whittaker, D. M. Confined Plasmons in Metallic Nanocavities. *Phys. Rev. Lett.* **2001**, *87*, 176801.

(18) Kelf, T. A.; Sugawara, Y.; Cole, R. M.; Baumberg, J. J.; Abdelsalam, M. E.; Cintra, S.; Mahajan, S.; Russell, A. E.; Bartlett, P. N. Localized and Delocalized Plasmons in Metallic Nanovoids. *Phys. Rev. B* **2006**, *74*, 245415.

(19) Cui, L.; Mahajan, S.; Cole, R. M.; Soares, B.; Bartlett, P. N.; Baumberg, J. J.; Hayward, I. P.; Ren, B.; Russell, A. E.; Tian, Z. Q. UV SERS at Well Ordered Pd Sphere Segment Void (SSV) Nanostructures. *Phys. Chem. Chem. Phys.* **2009**, *11*, 1023−1026.

(20) Yue, G. A Promising Method for Electrodeposition of Aluminium on Stainless Steel in Ionic Liquid. *AIChE J.* **2009**, *55*, 783−796.

(21) Hugall, J. T.; Finnemore, A. S.; Baumberg, J. J.; Steiner, U.; Mahajan, S. Solvent-Resistant Ultraflat Gold Using Liquid Glass. *Langmuir* **2012**, *28*, 1347−1350.

(22) Nagpal, P.; Lindquist, N. C.; Oh, S.-H.; Norris, D. J. Ultrasmooth Patterned Metals for Plasmonics and Metamaterials. *Science* **2009**, *325*, 594−7.

(23) Blackstock, J.-J. Fabrication and Characterization of Ultra-flat Thin-Film Material Surfaces for Nanoscale Research and Device Applications. Ph.D. Thesis, University of Alberta, Alberta, Canada, 2005.

(24) Dörfer, T.; Schmitt, M.; Popp, J. Deep-UV Surface-Enhanced Raman Scattering. *J. Raman Spectrosc.* **2007**, *38*, 1379−1382.

(25) Jha, S. K.; Ahmed, Z.; Agio, M.; Ekinci, Y.; Loffler, J. F. Deep-UV Surface-Enhanced Resonance Raman Scattering of Adenine on Aluminum Nanoparticle Arrays. *J. Am. Chem. Soc.* **2012**, *134*, 1966−1969.

(26) Li, L.; Fang Lim, S.; Puretzky, A. a.; Riehn, R.; Hallen, H. D. Near-Field Enhanced Ultraviolet Resonance Raman Spectroscopy using Aluminum Bow-Tie Nano-antenna. *Appl. Phys. Lett.* **2012**, *101*, 113116.

(27) Taguchi, A.; Hayazawa, N.; Furusawa, K.; Ishitobi, H.; Kawata, S. Deep-UV Tip-Enhanced Raman Scattering. *J. Raman Spectrosc.* **2009**, *40*, 1324−1330.

(28) Giese, B.; McNaughton, D. Surface-Enhanced Raman Spectroscopic and Density Functional Theory Study of Adenine Adsorption to Silver Surfaces. *J. Phys. Chem. B* **2002**, *106*, 101−112.

(29) Cui, L.; Wu, D.; Wang, A.; Ren, B.; Tian, Z. Charge-Transfer Enhancement Involved in the SERS of Adenine on Rh and Pd Demonstrated by Ultraviolet to Visible Laser Excitation. *J. Phys. Chem. C* **2010**, *114*, 16588−16595.

(30) Cole, R. M.; Mahajan, S.; Bartlett, P. N.; Baumberg, J. J. Engineering SERS via Absorption Control in Novel Hybrid Ni/Au Nanovoids. *Opt. Express* **2009**, *17*, 13298−308.